

# ***Numerical investigation of shot-noise suppression in diffusive conductors***

**Massimo Macucci**

Dipartimento di Ingegneria dell'Informazione: Elettronica, Informatica, Telecomunicazioni,  
Università di Pisa

**Giuseppe Iannaccone**

Dipartimento di Ingegneria dell'Informazione: Elettronica, Informatica, Telecomunicazioni,  
Università di Pisa

**Giovanni Basso**

Dipartimento di Ingegneria dell'Informazione: Elettronica, Informatica, Telecomunicazioni,  
Università di Pisa

**Bruno Pellegrini**

Dipartimento di Ingegneria dell'Informazione: Elettronica, Informatica, Telecomunicazioni,  
Università di Pisa

**Numerical investigation of shot-noise suppression in diffusive conductors**

M. Macucci, G. Iannaccone, G. Basso, and B. Pellegrini

*Dipartimento di Ingegneria dell'Informazione, Università degli studi di Pisa, Via Diotisalvi 2, I-56122 Pisa, Italy*

(Received 20 September 2002; revised manuscript received 31 December 2002; published 28 March 2003)

We present a numerical study of shot noise in diffusive mesoscopic conductors, aimed at a quantitative understanding of the conditions needed for achieving the  $1/3$  suppression factor predicted from random matrix theory. We investigate both two-dimensional and three-dimensional conductors, with a hard-wall model in which elastic scatterers are represented by randomly positioned obstacles. Finally, we discuss the effect on noise of obstacles of finite height, comparable with the Fermi level, and comment on the possibility of similar effects in wires obtained by means of electrostatic depletion in modulation doped semiconductor heterostructures.

DOI: 10.1103/PhysRevB.67.115339

PACS number(s): 73.23.-b, 72.70.+m, 72.20.-i, 73.63.Nm

**I. INTRODUCTION**

In the last few years, starting with the seminal article by Beenakker and Büttiker,<sup>1</sup> significant attention has been devoted in the physics community to the issue of shot-noise suppression in diffusive conductors, i.e., conductors in which transport is dominated by elastic scattering with the detailed features of the potential landscape. The condition of diffusive transport is realized when the length of the device  $L$  is larger than the mean-free-path  $l$  between elastic scattering events and smaller than the mean-free-path  $\lambda$  between inelastic scattering events. It has been shown<sup>1</sup> that, if the number of propagating modes  $N$  in the conductor is such that  $l \ll L \ll Nl$ , the current power spectral density of shot noise in a diffusive conductor is reduced by a factor  $1/3$  with respect to the “full shot” value  $2e|I|$  (where  $e$  is the electron charge and  $I$  is the average current through the device) that would be expected on the basis of Schottky’s formula<sup>2</sup> for Poissonian noise. Suppression of shot noise is a consequence of correlations between electrons crossing the device: while in the case of a Poissonian process crossing events are totally uncorrelated, introduction of an “antibunching” effect, i.e., making electron injection into the device less likely if another electron is occupying one of the propagating modes, leads to a decrease in the variance of the current and therefore to a reduced noise power spectral density. The authors of Ref. 1 have developed an approach based on random matrix theory, which allows them to establish that, due to the resulting binomial distribution of the transmission eigenvalues, the shot-noise suppression in a diffusive conductor is exactly  $1/3$ . Later demonstrations have been given by Nazarov,<sup>3</sup> Altshuler, Levitov, and Yakovets,<sup>4</sup> as well as by Blanter and Büttiker.<sup>5</sup> The same suppression factor has been obtained with a fully semiclassical approach by Nagaev.<sup>6</sup> All of these models focus on degenerate diffusive conductors, in which the prevalent interaction creating the correlations that lead to noise suppression is represented by Pauli exclusion.

Other authors have focused on the investigation of shot-noise suppression in nondegenerate diffusive conductors, in which Pauli exclusion plays a lesser role and correlations are substantially due to Coulomb interaction. In particular, González *et al.*<sup>7</sup> obtain a suppression factor  $1/3$  from a clas-

sical Monte Carlo simulation of a (3D) three-dimensional conductor in which the electrostatic potential is computed with a “dynamic” Poisson solver, i.e., with a procedure involving the determination of the instantaneous electrostatic potential due to all the electrons in the device at each time step. Shot-noise suppression in this case is dependent on the dimensionality  $d$  of the conductor, as confirmed also by the analytical results by Schomerus *et al.*,<sup>8</sup> and equals approximately  $1/d$ , with variations according to the dependence of the scattering time on energy that is assumed.

We shall however focus on the case of degenerate conductors and, specifically, on the analysis of our numerical results in relationship with the outcome of the calculations of Refs. 1,6. In particular, the coincidence between the  $1/3$  suppression factor from the quantum mechanical calculation of Ref. 1 and that yielded by the semiclassical approach of Ref. 6 had initially been considered surprising and possibly due to a numerical coincidence.<sup>9</sup> But it is now recognized<sup>10</sup> that this is just the result of the action of Pauli exclusion, which is included both in the quantum mechanical and in the semiclassical approaches, without any significant role played on the average quantities by coherence.

Our current model can handle up to 200 transverse modes, as a consequence of improved numerical precision and efficiency with respect to earlier numerical approaches.<sup>10</sup> The increased numerical efficiency allows us to overcome the limitations mentioned by Kolek, Stadler, and Haldaš,<sup>11</sup> in the simulation of the fully diffusive regime. The authors of Ref. 11 present an interesting numerical analysis of shot-noise suppression in the transition between ballistic and diffusive transports in a disordered conductor, as well as of the noise behavior in the weak and strong localization regimes. While they focus on the numerical verification of several theoretical expressions for the shot-noise suppression factor, and average over a large number of samples, we are more interested in obtaining data that can be directly compared with experiments, and therefore perform calculations for a single sample with a realistic size.

We compute the transmission matrix, by means of an optimized recursive Green’s function approach, in a model conductor containing a large number of randomly placed obstacles. From the transmission matrix, we obtain the shot-

noise suppression factor in a variety of conditions and for two- and three-dimensional conductors. We extend our analysis also to the condition of “soft scatterers,” i.e., obstacles that are not completely opaque for the impinging electrons, and discuss the results in relationship with the available experimental data on shot noise for diffusive transport in semiconductors.<sup>12</sup> Although such experimental data are not conclusive, significant deviations seem to occur from the 1/3 suppression, which is instead confirmed almost exactly in the case of measurements on metallic diffusive conductors.<sup>13</sup>

In Sec. II we present the model of a diffusive conductor that we have used for our simulations, the numerical procedure implemented for the calculation of the transmission and reflection matrices, and the problem size limitations. Numerical results are reported in Sec. III, and discussed with reference to the existing literature. Finally, conclusions and perspectives for further work are presented in Sec. IV.

## II. MODEL

We model the conductor as a wire defined by hard walls, with a flat bottom and containing a number of obstacles that are spread according to a uniform random distribution. The technique that we apply to compute the transmission and reflection matrices can handle a generic potential landscape, but we have decided to focus on a hard-wall approximation, which limits the size of the parameter space and yields results that do not exhibit significant qualitative differences with respect to those for more elaborate potential profiles.

The obstacles, to which in the following we will refer also as “scatterers,” are square (or cubic, in the 3D model) regions, where the potential has a value larger than that of the “flat bottom” of rest of the wire. If the potential associated with the scatterers is much larger than the Fermi energy, they are opaque, i.e., they represent real hard obstacles for electron propagation. Otherwise, for “heights” of the scatterers comparable to the Fermi energy or even smaller, they act simply as perturbations of the potential in which the electrons propagate. In any case, obstacles of any height act as elastic scatterers, since no energy dissipation mechanism is included. Location of the obstacles is decided generating pairs (or triplets in the 3D case) of independent, uniformly distributed random variables, which represent the cartesian coordinates of their centers.

For the 2D model we choose the direction of current flow along  $x$ , and the  $y$  axis is therefore in the transverse direction. In this case the random variable corresponding to the  $x$  coordinate is uniformly distributed between 0 and  $L$ , the length of the wire, while the random variable for the  $y$  coordinate is uniformly distributed between 0 and  $W$ , the wire width. In the 3D model the direction of current propagation is again along  $x$ , while  $y$  and  $z$  are the coordinates of the transverse cross section. Obstacles for the 3D wire are positioned generating three random variables for the  $x$ ,  $y$ , and  $z$  coordinates, which are uniformly distributed in the intervals  $[0, L]$ ,  $[0, W]$ ,  $[0, H]$ , respectively, where  $H$  is the height of the wire along  $z$ . Both for the 2D and the 3D cases, the possible

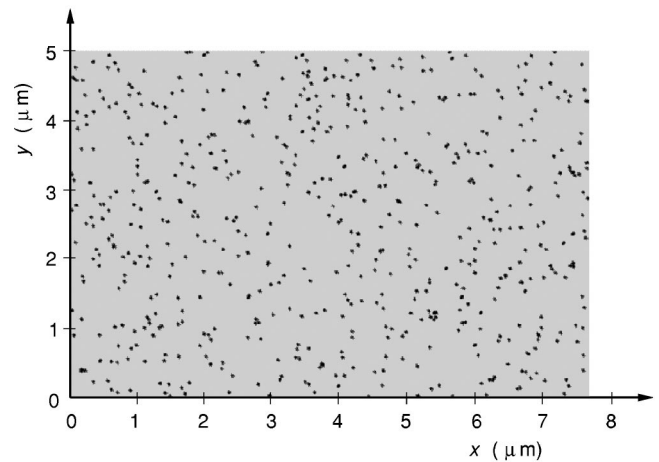


FIG. 1. Potential landscape in a diffusive conductor  $7.72 \mu\text{m}$  long,  $5 \mu\text{m}$  wide, containing 600 randomly distributed square  $25 \times 25 \text{ nm}^2$  hard-wall scatterers. Black indicates an infinite potential and light gray indicates zero potential.

coordinates of the obstacle centers are restricted to a discrete set of values, rounding the results obtained for the random variables from a linear congruence generator. The need for such a discretization will become apparent when we describe the procedure for the calculation of the transmission matrix. In Fig. 1 we show a typical obstacle distribution for a 2D wire. For this example we have  $L = 7.72 \mu\text{m}$ ,  $W = 5 \mu\text{m}$  and a number  $M = 600$  of square obstacles, each of which with a size of  $25 \times 25 \text{ nm}^2$ . The diffusive section of the wire is connected to semi-infinite leads of the same width, without obstacles, and in which transport is thus ballistic.

For the calculation of the transmission and reflection matrices we have adopted a technique based on a development of the recursive Green’s function formalism<sup>14</sup> that has specific advantages, which will be discussed in the following, for this particular problem. The wire is subdivided into a number of transverse “slices,” in each of which the potential is constant along the longitudinal direction. It is straightforward to compute the Green’s functions for propagation along each of these sections, with the assumption of Dirichlet boundary conditions at their ends.<sup>15</sup> With such boundary condition, each section is separated from the others: we need to define a procedure to obtain, from the Green’s functions of the isolated sections, the Green’s functions of two coupled adjacent sections. This is achieved by considering coupling between the two sections as a perturbation  $V$ , and computing the perturbed Green’s functions via the Dyson equation. Such a procedure is repeated recursively, adding one slice at a time, until the input lead is reached. The details of the method are described in Refs. 15,16.

At the end of the recursive procedure, we have available the Green’s function matrix  $G_{oi}$  between a slice in the input lead and a slice in the output lead, as well as that  $G_{ii}$  between a slice in the input lead and itself. From them, the transmission  $t$  and reflection  $r$  matrices can be obtained with the straightforward procedure of Ref. 15.

The recursive Green’s function approach is particularly convenient for the solution of the open-boundary Schröd-

dinger equation in a structure such as a diffusive wire, in which we need to consider a very large number of slices, due to the fine scale on which the confinement potential fluctuates. Requirements for numerical stability in the presence of many evanescent modes rule out techniques such as the transfer-matrix method. Approaches such as those based on the recursive calculation of the scattering matrix,<sup>17</sup> although formally very close to our Green's function technique, do require some additional attention if each of the elementary scattering matrices is computed using mode matching at the interface between adjacent sections, in the presence of opaque scatterers. Opaque scatterers are equivalent to hard-wall conditions, which need to be handled with particular care, as far as the matching conditions for the normal derivative are concerned,<sup>18</sup> and this leads to undesired complications for a structure with a possibly rather complex geometry at each interface.

Even with our recursive Green's function method, the investigation of a conductor in the diffusive regime poses very strict requirements on the numerical precision, since quite a large number of transverse slices must be included, in order to satisfy the condition  $L \gg l$ , and, at the same time, a very large number of transverse modes must be considered for each slice, to make sure that  $Nl \gg L$ , as discussed also in Ref. 11. Significant improvements were needed with respect to the code used for the calculations of Refs. 10,16. The present version of our code can handle structures with up to 200 transverse modes and 1600 slices.

Let us finally discuss the procedure that we follow to compute the shot-noise suppression factor. By definition, such a suppression factor, also referred to as "Fano factor," corresponds to the ratio of the actual shot noise power spectral density  $S_I$  to that of full shot-noise  $S_I^{\text{fs}}$  expected from Schottky's theorem,

$$\gamma = \frac{S_I}{S_I^{\text{fs}}} = \frac{S_I}{2eI}. \quad (1)$$

The shot-noise power spectral density is given by the expression<sup>19</sup>

$$S_I = 4 \frac{e^2}{h} |eV| \text{Tr}[t^\dagger t (I - t^\dagger t)], \quad (2)$$

which, exploiting the invariance properties of the trace of a matrix for rotations, becomes

$$S_I = 4 \frac{e^2}{h} |eV| \sum_i T_i (1 - T_i), \quad (3)$$

where  $T_i$  is the  $i$ th eigenvalue of  $t^\dagger t$ . Since, from the Landauer-Büttiker formula, the conductance is given by

$$G = 2 \frac{e^2}{h} \sum_i T_i, \quad (4)$$

the Fano factor can be computed from

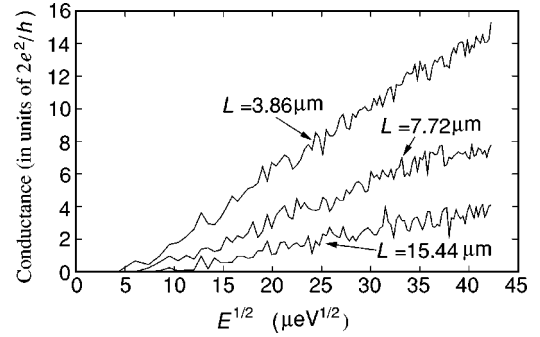


FIG. 2. Conductance of three diffusive 2D conductors of different length as a function of the Fermi energy of the impinging electrons. All conductors are  $5 \mu\text{m}$  wide and contain a uniform distribution of  $25 \times 25 \text{ nm}^2$  hard-wall scatterers, with a density of  $15.5521 \mu\text{m}^{-2}$ .

$$\gamma = \frac{\sum_i T_i (1 - T_i)}{\sum_i T_i}, \quad (5)$$

which can be directly implemented in the numerical calculations.

### III. RESULTS

We have tested the validity of our model for a diffusive conductor, verifying, in particular, the dependence of conductance on length. To this aim, we have computed the conductance for two-dimensional diffusive wires that are  $3.86 \mu\text{m}$ ,  $7.72 \mu\text{m}$ ,  $15.44 \mu\text{m}$  long. For all three conductors the width is  $5 \mu\text{m}$  and the obstacles are square, with a side of  $25 \text{ nm}$  and a density of  $15.55 \mu\text{m}^{-2}$ . Results for the conductance in the three cases are reported in Fig. 2, as a function of the square root of the Fermi energy. Since we are considering hard-wall confinement, the number of propagating modes in the wire is proportional to the square root of the energy (the energy eigenvalues for a square well have a quadratic dependence on the eigenmode order), and therefore such a number increases linearly with the abscissa of our plot. The conductance is roughly proportional to the number of propagating modes, and therefore it exhibits a linear increase in our plots, although its quantization has been washed out by the diffusive behavior, which is confirmed by the fact that, for a given value of the Fermi energy, the conductance is also inversely proportional to conductor length. From knowledge of the conductance, we can obtain an estimate of the mean-free path between elastic-scattering events, using a Drude-like model,<sup>20</sup> according to which, for a 2D conductor,

$$G = \frac{G_0 N}{L} \frac{\pi l}{2}, \quad (6)$$

where  $G_0$  is the conductance quantum  $2e^2/h$ . There are 91 propagating modes for the largest value of the Fermi-energy shown in Fig. 2; substituting the values for the wire length

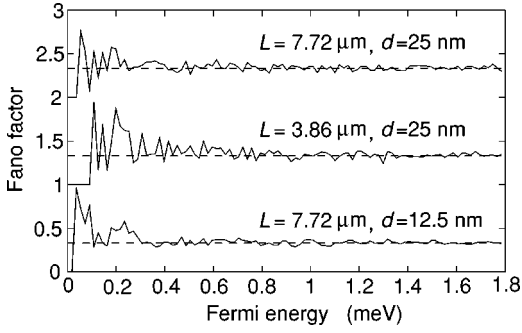


FIG. 3. Fano factor as a function of the Fermi energy of the impinging electrons for three different samples. The top curve refers to a wire with a length of  $7.72 \mu\text{m}$ , with  $25 \times 25 \text{ nm}^2$  scatterers, the middle curve is for a wire  $3.86 \mu\text{m}$  long, with  $25 \times 25 \text{ nm}^2$  scatterers, and the bottom curve is for a  $7.72 \mu\text{m}$  wire with  $12.5 \times 12.5 \text{ nm}^2$  scatterers. For all three cases the number of scatterers is 600. The different curves are vertically shifted by 1 for the sake of presentation clarity. We have added also dashed lines in correspondence with the value  $1/3$ .

and the conductance into Eq. (6), we get  $l = 0.43 \mu\text{m}$ . Therefore, the condition  $L \gg l$  is certainly satisfied, as well as the condition  $Nl \gg L$ , at least for the shortest wire and for the largest values of the energy.

In Fig. 3 we report the Fano factor as a function of the Fermi energy for three wires  $5 \mu\text{m}$  wide; curves are vertically shifted by 1 for clarity of presentation, and dashed lines indicate the value  $1/3$ . The top curve is for a wire with a length of  $7.72 \mu\text{m}$ , with 600 square  $25 \times 25 \text{ nm}^2$  obstacles. The middle curve is for a wire  $3.86 \mu\text{m}$  long, containing 600 square  $25 \times 25 \text{ nm}^2$  obstacles. Finally, the bottom curve is for a wire  $7.72 \mu\text{m}$  long, with 600 square  $12.5 \times 12.5 \text{ nm}^2$  obstacles. We notice that for a large enough Fermi energy all three curves converge to the expected value  $1/3$ . Actually, the value  $1/3$  is reached as soon as the number of propagating modes is about 3 times the ratio  $L/l$ . Let us provide estimates of  $Nl$  in correspondence with the values of the Fermi energy for which the Fano factor settles around  $1/3$  in the three cases of Fig. 3. For the top curve, we notice that the asymptotic behavior starts at about  $0.6 \text{ meV}$ , corresponding to 52 propagating modes. Since the value of  $l$  was previously found to be  $0.43 \mu\text{m}$ , we obtain  $Nl = 22.36 \mu\text{m}$ , corresponding to 2.89 times the length  $L$ . For the middle curve, we can assume that an asymptotic condition is achieved for a Fermi energy of about  $0.85 \text{ meV}$ , corresponding to 62 propagating modes. Since in this case the elastic mean-free path is around  $0.162 \mu\text{m}$ , we obtain  $Nl = 10.04 \mu\text{m}$ , which is 2.6 times the device length. Finally, for the bottom curve, we notice that a value of  $\approx 1/3$  is achieved around a Fermi energy of about  $0.4 \text{ meV}$ , corresponding to 36 propagating modes, and therefore to  $Nl \approx 20 \mu\text{m}$ , which equals the wire length times 2.6.

As already mentioned in the previous sections, we have extended the analysis of shot-noise suppression also to the case of higher dimensionality, and, in particular, to the case of a 3D conductor consisting in a wire with a square cross section of  $0.5 \times 0.5 \mu\text{m}$  and a length of  $10 \mu\text{m}$ . In Fig. 4 the Fano factor for such a structure has been plotted for a total

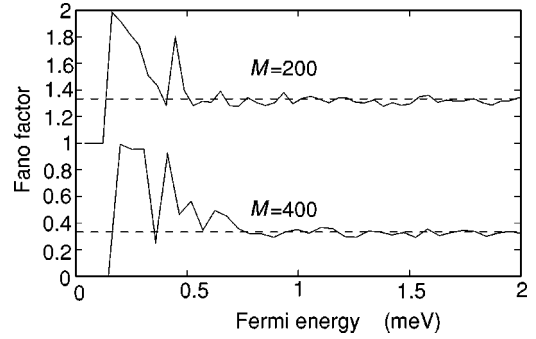


FIG. 4. Fano factor as a function of the Fermi energy for three-dimensional wires with a  $0.5 \times 0.5 \mu\text{m}$  square cross section and a length of  $10 \mu\text{m}$ . The wires contain 200 (upper plot) or 400 (lower plot) randomly placed cubic hard-wall obstacles with a side of  $50 \text{ nm}$ . A vertical shift of 1 unit has been added to the upper plot to improve readability. The dashed lines correspond to the expected asymptotic value of  $1/3$ .

number  $M$  of obstacles of 200 (upper plot) or 400 (lower plot). Obstacles are cubic, with a side of  $50 \text{ nm}$ , and randomly distributed. Based on the previously considered Drude-like model,<sup>20</sup> in 3D the mean-free path between elastic scattering events is given by

$$l_{3D} = \frac{G}{G_0} \frac{3L}{4N}. \quad (7)$$

For a Fermi energy of  $2 \text{ meV}$ , we have a conductance of  $10.8 G_0$  for the case with 200 obstacles and of  $8.4 G_0$  for the case with 400 obstacles. In both cases the number of propagating modes is 80, therefore, we obtain a mean-free path between elastic-scattering events  $l_{3D} = 1.013 \mu\text{m}$  for the wire with 200 obstacles and  $l_{3D} = 0.788 \mu\text{m}$  for the wire with 400 obstacles.

We observe that in the upper plot of Fig. 4 the Fano factor settles around the value  $1/3$  for a Fermi-energy  $E_F$  of  $\approx 0.6 \text{ meV}$ , corresponding to about 19 propagating modes, therefore, as soon as  $Nl_{3D} \approx 2L$ ; for the lower plot this happens for  $E_F \approx 0.8 \text{ meV}$ , corresponding to about 26 propagating modes, and thus again to the condition  $Nl_{3D} \approx 2L$ . Hence, the conditions for reaching the asymptotic behavior in a 3D sample are very similar to those previously discussed for the 2D case.

The results shown so far have been obtained assuming hard-wall obstacles as scatterers: this assumption, however, does not faithfully reproduce, for example, the scattering action due to ionized donors in a conductor defined by selectively depleting a two-dimensional electron gas (2DEG) created by modulation doping. In such a case, the donors are located in the donor layer, which is physically separate from the 2DEG and give rise to “bumps” in the potential seen by the 2DEG electrons, rather than to hard obstacles. It is, therefore, interesting to see what happens to the Fano factor for our model in the presence of scatterers of finite height. We have considered 3 values for the obstacle height  $h$ : 1, 5, and 25 meV, for a conductor  $5 \mu\text{m}$  wide,  $7.72 \mu\text{m}$  long and containing 600 square  $25 \times 25 \text{ nm}^2$  obstacles. Results are reported in Fig. 5: for the lowest obstacle height, which is less than the largest values of the Fermi-energy considered, the

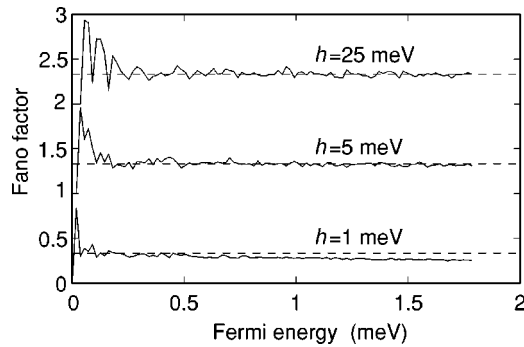


FIG. 5. Fano factor as a function of the Fermi energy of the impinging electrons for a wire  $5 \mu\text{m}$  wide,  $7.72 \mu\text{m}$  long, containing 600 square  $25 \times 25 \text{ nm}^2$  obstacles with a height of 1, 5, or 25 meV. The dashed lines indicate the diffusive limit of  $1/3$ .

Fano factor drops significantly below the value  $1/3$ . This is expected, if we consider that, as the energy increases over the height of the obstacles, their scattering action is significantly reduced, the transmission coefficients increase, and we move toward the purely ballistic regime with unitary transmission, in which shot noise vanishes. For the obstacles that are 5 meV high, we observe a trend toward a drop only for the largest values of the Fermi energy, while for the 25-meV obstacles no relevant difference is visible with respect to the hard-wall case.

Estimation of shot-noise suppression with a realistic, self-consistent model of a quantum wire defined in a semiconductor heterostructure is beyond the scope of the present paper, but the result for soft-wall obstacles provides a hint of why experimental verification of shot-noise suppression to the  $1/3$  diffusive limit has been elusive so far. The only existing noise measurement on a potentially diffusive quantum wire<sup>12</sup> has yielded results that are not conclusive, with a Fano factor that has a significant dependence on the gate bias. Since variations of the bias applied to the gates defining the quantum wire lead to a change in the relative position of the Fermi level and of the potential fluctuations due to the ionized donors. A dependence of shot-noise suppression on gate bias is to be expected, based on our results, although a quantitative prediction requires a detailed model of the wire, which is currently under development.

Finally, we have studied the effect that the lateral dimension of the obstacles has on shot-noise suppression. The extension of the obstacles plays a role similar to their height. If the obstacles are too small, their scattering cross section is not sufficient to guarantee a mean-free path much smaller than the device length, and therefore shot noise tends to decrease below the  $1/3$  limit. In Fig. 6, we present the Fano factor computed for three wires  $5 \mu\text{m}$  wide,  $7.72 \mu\text{m}$  long and containing 300 square randomly placed obstacles with a side  $d$  of 25, 50, 100 nm. It is apparent that for  $d=100$  nm the diffusive limit is achieved and maintained in the whole range of energies considered, while for  $d=50$  nm there is a very slight trend toward a decrease below  $1/3$ , and for  $d=25$  nm we have a clear drop of the Fano factor as soon as the energy is larger than about 0.5 meV. If we evaluate the mean-free path by means of Eq. (6), using the conductance

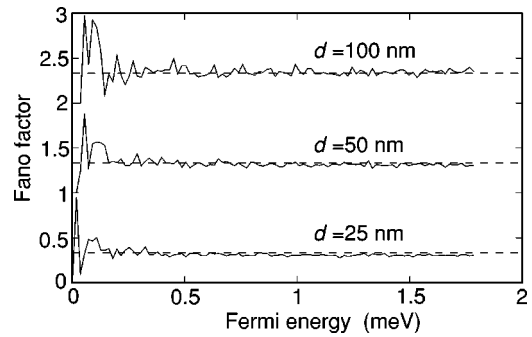


FIG. 6. Fano factor as a function of the Fermi energy of the impinging electrons for a wire  $5 \mu\text{m}$  wide,  $7.72 \mu\text{m}$  long, containing 300 hard-wall square obstacles with a side  $d$  of 25, 50, and 100 nm. The dashed lines indicate the diffusive limit of  $1/3$ .

values obtained from our simulation, we obtain  $l = 0.34 \mu\text{m}$  for  $d=100$  nm,  $l=0.72 \mu\text{m}$  for  $d=50$  nm, and  $l=0.87 \mu\text{m}$  for  $d=25$  nm. From these results we get an indication that, in order to reach the  $1/3$  limit, the conductor length  $L$  must be at least 10 times the mean-free-path  $l$ .

#### IV. CONCLUSION

We have presented a numerical investigation of shot-noise suppression in conductors containing randomly located elastic scatterers, focusing on the conditions for the achievement of the diffusive limit for which random matrix theory predicts a Fano factor of  $1/3$ . By means of a numerical model capable of treating up to 200 propagating transverse modes and based on the recursive Green's function formalism, we have investigated both 2D and 3D structures, obtaining, regardless of dimensionality, a suppression factor fluctuating, due to interference effects, around  $1/3$  as soon as the mean-free-path  $l$  between elastic scattering events is less than about a tenth of the conductor length  $L$ , and, at the same time, the product  $Nl$  of the number of propagating modes times  $l$  is larger than 2–3 times the conductor length.

With our model, we observe the transition from a complex noise behavior with few propagating modes to the  $1/3$  shot-noise suppression of the diffusive regime with tens of propagating modes. Our results provide further support to the argument<sup>10</sup> that the identity between the shot-noise suppression factor values found with a fully quantum mechanical model based on random matrix theory and with a semiclassical approach including Pauli exclusion is not a numerical coincidence, but a direct consequence of the convergence of quantum mechanical results to those of classical mechanics for conductors in which a large number of transverse modes can propagate. Such a convergence implies that phase coherence has no effect on noise properties in a situation with many propagating modes. It has recently been shown,<sup>21</sup> in the case of chaotic cavities, that the quantum-mechanical and the semiclassical results coincide even for higher-order cumulants of current fluctuations.

We have investigated shot-noise suppression also in the case of soft-wall scatterers, and concluded that, as soon as

the obstacle height becomes of the order of the Fermi energy, the Fano factor starts decreasing below the  $1/3$  diffusive limit, as could be expected, since we move from the diffusive regime toward the ballistic regime. In particular, this suggests that in a quantum wire defined by means of electrostatic depletion in a modulation doping heterostructure, it may be difficult to achieve the diffusive regime, due to the limited height of the potential perturbations, mainly caused by the donor ions, with respect to the Fermi level. A detailed

investigation of this issue requires a rather large computational model and is currently ongoing.

#### ACKNOWLEDGMENTS

This work has been supported by the Italian National Research Council (CNR) through the “5% Nanotecnologie” program and through the Madess II program, and by the co-funding program of the University of Pisa for the project “Excess noise in nanostructured materials and devices.”

- 
- <sup>1</sup>C.W.J. Beenakker and M. Büttiker, Phys. Rev. B **46**, 1889 (1992).  
<sup>2</sup>W. Schottky, Ann. Phys. (Leipzig) **57**, 541 (1918).  
<sup>3</sup>Yu.V. Nazarov, Phys. Rev. Lett. **73**, 134 (1994).  
<sup>4</sup>B.L. Altshuler, L.S. Levitov, A.Yu. Yakovets, Pis'ma Zh. Éksp. Teor. Fiz. **59**, 821 (1994) [JETP Lett. **59**, 857 (1994)].  
<sup>5</sup>Ya.M. Blanter and M. Büttiker, Phys. Rev. B **56**, 2127 (1997).  
<sup>6</sup>K.E. Nagaev, Phys. Lett. A **169**, 103 (1992).  
<sup>7</sup>T. González, C. González, J. Mateos, D. Pardo, L. Reggiani, O.M. Bulashenko, and J.M. Rubì, Phys. Rev. Lett. **80**, 2901 (1998).  
<sup>8</sup>H. Schomerus, E.G. Mishchenko, and C.W.J. Beenakker, Phys. Rev. B **60**, 5839 (1999).  
<sup>9</sup>R. Landauer, Microelectron. Eng. **47**, 7 (1999).  
<sup>10</sup>M. Macucci, G. Iannaccone, B. Pellegrini, in *Proceedings of the 15th International Conference on Noise in Physical Systems and 1/f Fluctuations, Hong Kong, 1999 (ICNF 99)*, edited by C. Surya (Bantham, London, 1999), p. 325.  
<sup>11</sup>A. Kolek, A.W. Stadler, and G. Haldaš, Phys. Rev. B **64**, 075202 (2001).  
<sup>12</sup>F. Liefrink, J.I. Dijkhuis, M.J.M. de Jong, L.W. Molenkamp, and H. van Houten, Phys. Rev. B **49**, 14 066 (1994).  
<sup>13</sup>M. Henny, S. Oberholzer, C. Strunk, and C. Schönenberger, Phys. Rev. B **59**, 2871 (1999).  
<sup>14</sup>P.A. Lee and D.S. Fisher, Phys. Rev. Lett. **47**, 882 (1981).  
<sup>15</sup>F. Sols, M. Macucci, U. Ravaioli, and Karl Hess, J. Appl. Phys. **66**, 3892 (1989).  
<sup>16</sup>M. Macucci, A. Galick, and U. Ravaioli, Phys. Rev. B **52**, 5210 (1995).  
<sup>17</sup>R.L. Schult, H.W. Wyld, and D.G. Ravenhall, Phys. Rev. B **41**, 12 760 (1990).  
<sup>18</sup>M. Macucci and Karl Hess, Phys. Rev. B **46**, 15 357 (1992).  
<sup>19</sup>M. Büttiker, Phys. Rev. Lett. **65**, 2901 (1990).  
<sup>20</sup>M. J. M. de Jong and C. W. J. Beenakker, in *Coulomb and interference effects in small electronic structures*, edited by D. C. Glatli, M. Sanquer, and J. Trân Than Vân (Edition Frontières, France, 1994).  
<sup>21</sup>K.E. Nagaev, P. Samuelsson, and S. Pilgram, Phys. Rev. B **66**, 195318 (2002).